Specific heat of thin phonon cavities at low temperature: Very high values revealed by zeptojoule calorimetry

Adib Tavakoli,[1,2] Kunal J. Lulla,[1,2] Tuomas Puurtinen,[3] Ilari Maasilta,[3] Eddy Collin,[1,2]
Laurent Saminadayar,[1,2] and Olivier Bourgeois[1,2]
[1]*Institut Néel, CNRS, 25 avenue des Martyrs, F-38042 Grenoble, France*
[2]*Université Grenoble Alpes, Institut Néel, F-38042 Grenoble, France*
[3]*Nanoscience Center, Department of Physics, University of Jyväskylä, P.O. Box 35, FI-40014 Jyväskylä, Finland*

(Received 9 February 2022; revised 24 May 2022; accepted 14 June 2022; published 27 June 2022)

The specific heat of phonon cavities is investigated in order to analyze the effect of phonon confinement on thermodynamic properties. The specific heat of freestanding very thin SiN membranes in the low-dimensional limit is measured down to very low temperatures (from 6 K to 50 mK). In the whole temperature range, we measured an excess specific heat orders of magnitude bigger than the typical value observed in amorphous solids. Below 1 K, a crossover in c_p to a lower power law is seen, and the value of the specific heat of thinner membranes becomes larger than that of thicker ones demonstrating a significant contribution coming from the surface. We show that this high value of the specific heat cannot be explained by the sole contribution of two-dimensional phonon modes (Lamb waves). The excess specific heat, being thickness dependent, could come from tunneling two-level systems that form in low-density regions of amorphous solids located on the surfaces. We also show that the specific heat is strongly tuned by the internal stress of the membrane by orders of magnitude, giving high values, making low-stress SiN very efficient for energy storage at very low temperature.

DOI: 10.1103/PhysRevB.105.224313

I. INTRODUCTION

The thermal properties of low-dimensional amorphous material nanowires, membranes, etc., are at the heart of essential questions for many subjects such as bolometry, temperature sensing, or simply the understanding of phonon physics at very low temperature in dielectric nanosystems [1]. Even if the thermal transport in low-dimensional dielectric nanostructures has recently been the subject of numerous although difficult experiments at subkelvin temperatures [2–5], the specific heat, or the capacity of a body to rise in temperature following a supplied external energy, remains very poorly understood and experimentally almost unexplored [6].

At very low temperatures, two significant physical effects are expected to impact the thermal properties of thin membranes, pushing the value of the specific heat far from that of a conventional three-dimensional (3D) solid material. The first is the effect of the confinement of the phonon modes in nanostructures thinner than the wavelength of phonons. In that kind of freestanding membrane, it is expected that new phonon modes will appear having quadratic and not linear dispersion relations, modes whose contribution to the specific heat at low temperature is linear in T [6–12]. Such modes have been experimentally observed in the thermally relevant hypersonic frequency range [13]. Note that simple arguments would have naively predicted that the specific heat of a confined phonon gas in the low-temperature limit should scale with T^{δ}, δ being the effective dimension of the considered system (for a suspended membrane $\delta = 2$ at low enough temperature).

Secondly, it is well known that the thermal behavior of amorphous (glassy) materials differs significantly from their crystalline counterparts. For more than 40 years, the thermal properties of such glassy materials have been explained by the possible presence of dynamic defects acting as tunneling two-level systems (TLSs) [14–16]. Below a certain temperature, usually around 1 K, these defects add a sizable contribution to the specific heat through additional degrees of freedom providing also a linear variation of c_p with temperature. These dynamic defects are expected to scatter phonons, thus acting on the thermal transport of such low-dimensional structures [4,5].

Consequently, very particular behavior of the phonon specific heat is expected at very low temperature in quasi-2D self-suspended amorphous materials. Such systems should thus allow us to address the question of the main mechanism governing the thermal properties of confined glassy material when it moves from a standard system described by continuum elastic theory to a system dominated by TLSs, as well as the question of how the internal characteristics of an amorphous material such as stress can influence thermal properties [17–19]. Apart from the fundamental aspect of differentiating between the two theoretical models, since specific heat governs the characteristic time scales of low-temperature thermal detectors, which often employ suspended ultrathin membranes, it is essential to solve this controversy by doing direct experiments on them.

Here, we report highly sensitive specific heat measurements of thin membranes in the quasi-2D limit. They were

performed on thin silicon nitride suspended structures at subkelvin temperatures using zeptojoule calorimetry. By comparing results obtained for two different thicknesses (100 and 300 nm), it is shown that above 1 K the specific heat is dominated by 3D bulk contributions whereas for $T < 1$ K surface contributions dominate. Moreover, even if we observe a close-to-linear behavior of the specific heat as a function of the temperature below 1 K, we show that the "standard' ' elastic continuum model (Lamb modes) cannot explain even the order of magnitude of the measured specific heat. The presence of TLSs in the amorphous dielectric material is the most probable scenario to explain this anomalously high specific heat. The absolute value of the specific heat measured in our experiment is *up to five orders of magnitude* larger than that measured in a crystalline bulk material, making the used SiN thin membranes the system with the largest specific heat in this range of temperatures.

II. EXPERIMENTAL SET-UP

The specific heat of suspended thin membranes of silicon nitride has been measured down to very low temperatures using a highly sensitive technique. Various types of silicon nitride films have been used to fabricate the sensors: stoichiometric Si_3N_4 that has a high internal tensile stress of 0.95 GPa and two nonstoichiometric silicon nitrides, one of which has a low stress (0.2 GPa) and one of which has a super low stress (<0.1 GPa). We used 100- and 300-nm-thick commercially available SiN films deposited by a low-pressure chemical vapor process on top of a Si substrate. These thicknesses have been chosen to be of the same order of magnitude as the dominant phonon wavelength to ensure that only the 2D phonon modes are occupied in the membrane. Here, we define the dominant phonon wavelength λ_{dom} to correspond to the wavelength at which the Planck distribution (spectral energy density per volume) for bosons is maximum [20]. For 3D phonons, the dominant phonon wavelength is given by

$$\lambda_{\mathrm{dom}} = \frac{h v_{s,i}}{2.82 k_B T}, \tag{1}$$

with $v_{s,i}$ being the velocity of sound for mode i, h being the Planck constant, and k_B being the Boltzmann constant; for SiN, $v_s = 10\,000$ m/s and $\lambda_{\mathrm{dom}} = 100$ nm around 1 K. By fabricating 100-nm-thick membranes, the 2D phonon regime for thermal properties should be accessible at the lowest temperature of the experiment (below 0.1 K).

The thermal sensor is made of a self-supported SiN membrane of size 40×40 μm defining the dimensions of the quasi-2D phonon cavity suspended by eight arms (6 μm wide and 100 μm long). The long suspending arms lead to a very good thermal insulation of the membranes from the Si frames [5]. These arms serve also as mechanical support for the electrical leads of the transducers (see Fig. 1). A copper heater and a niobium nitride (NbN) thermometer are structured by laser lithography on the SiN membrane as shown in Fig. 1(a); the electrical leads are made with superconducting materials (NbTi). The temperature coefficient of resistance of the NbN calculated through $\alpha = \frac{1}{R}\frac{dR}{dT}$ can be higher than -1 K^{-1}, a particularly high value for thin film technology [21].

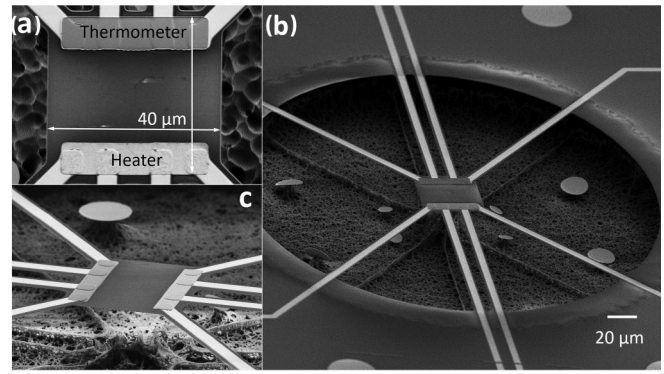

FIG. 1. Suspended membrane-based zeptojoule nanocalorimeter. (a) A top view of the 2D nanocalorimeter made of amorphous SiN that is functionalized with two transducers: a heater and a thermometer. (b) and (c) Angled views of the nanocalorimeter, which is suspended from eight suspension beams.

An example of a measurement of heat capacity is presented in Fig. 2. It is measured using an ac-calorimetry technique, a dynamic method based on modulating the temperature that is efficient and highly sensitive especially at low temperatures. In recent papers [22–25], we have demonstrated on these sensors a sensitivity for specific heat measurement of 2×10^{-16} J K^{-1} $\sqrt{\mathrm{Hz}}^{-1}$, for an oscillation of temperature of 3 mK, giving a sensitivity in energy of $\pm 10^{-19}$ J/$\sqrt{\mathrm{Hz}}$, i.e., $\pm$100 zJ per $\sqrt{\mathrm{Hz}}$ at 100 mK. The sample holder is installed in a vacuum chamber ($<2 \times 10^{-6}$ mbar before cryopumping) on a stage regulated with a precision better than 20 μK at a temperature of 100 mK measured using a calibrated Speer carbon thermometer [21]. This setup allows the measurement of the specific heat of 2D phonon cavities from below 100 mK to above 7 K as can be seen in Fig. 2.

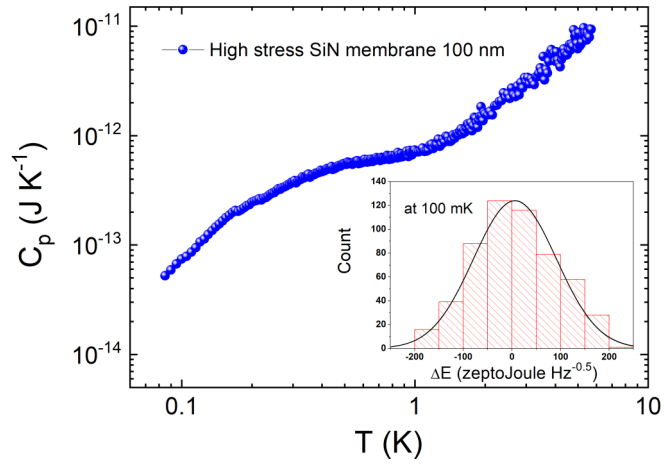

FIG. 2. Heat capacity of a 100-nm-thick membrane made out of high-stress Si_3N_4. The measurement of the heat capacity is shown over the temperature range 0.07–7 K. The noise has been measured at 100 mK as shown in the inset. The full width at half maximum shows that the measurement is done with a sensitivity in energy of $\pm$100 zJ.

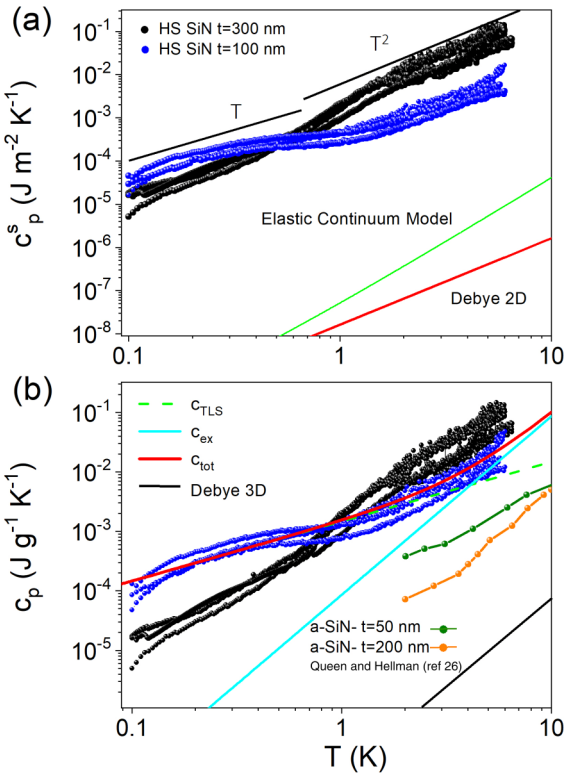

FIG. 3. The specific heat of thin membranes made of high-stress (HS) Si_3N_4. (a) The heat capacity normalized by the surface area of the membranes, in comparison to the predicted specific heat for a 2D phonon cavity for two sets of membranes of thicknesses 100 and 300 nm. The green line is the prediction of elastic continuum theory, and the red line is the Debye 2D model. The two black straight lines are guides to the eye for the temperature power laws T and T^2. (b) The heat capacity normalized by volume; same data as in (a). The cyan line is the excess specific heat c_{ex} from Eq. (6), the green dashed line is the specific heat of TLSs $c_{\mathrm{TLS}} \propto T$, and the red line is the total estimated specific heat from the sum of Eqs. (5) and (6) for an amorphous solid from which the TLS density is extracted. The black line is the predicted specific heat from the Debye 3D model. The green and orange dots are the specific heat of amorphous SiN (a-SiN) of thickness 50 and 200 nm, respectively, measured by Queen and Hellman [26], plotted for comparison.

III. RESULTS AND DISCUSSION

Specific heat measurements performed on two sets of membranes of high-stress SiN of thicknesses 100 and 300 nm are presented in Fig. 3 in different units: (1) in units normalized by the surface area $\mathrm{J\,m^{-2}\,K^{-1}}$, highlighting the surface effects, in Fig. 3(a), and (2) in the regular units $\mathrm{J\,g^{-1}\,K^{-1}}$ for volumetric specific heat, highlighting bulk effects, in Fig. 3(b). As expected, the specific heat (surface or volumetric) decreases when lowering the temperature as fewer and fewer degrees of freedom are excited. The total heat capacity signal is dominated by the SiN membrane contribution, as the heat capacities of the copper heater and the NbN thermometer are at least two orders of magnitude smaller over the whole temperature range of the experiments and will be neglected in the following discussion.

If we focus first on the low-temperature part, one clearly sees that below 1 K, both thin and thick membranes have approximately the same surface specific heat [see Fig. 3(a)], whereas in the high-temperature limit (above 1 K), it is the specific heat per unit volume which is almost identical for both types of samples [see Fig. 3(b)]. This indicates that in the low temperature range, the specific heat of the samples seems to be governed by the surfaces, whereas at higher temperatures, the specific heat is dominated by volumetric effects. One basis for interpretation resides in comparing the thickness of the samples with the dominant wavelength of the phonons. Indeed, a possible change between a 3D volume effect and a 2D surface effect arises when the phonon dominant wavelength becomes bigger than the membrane thickness. As mentioned earlier, by using Eq. (1), we obtained that λ_{dom} is on the order of a few hundreds of nanometers around 1 K. One can conclude that at temperatures lower than that the phonon specific heat is dominated by the lowest 2D phonon modes, as their wavelength is much larger than the thickness of the sample. As the temperature increases, λ_{dom} decreases, and one recovers the standard three-dimensional behavior for the specific heat. Considering these two limits, we can infer that we expect a 2D-3D crossover in the specific heat in this system, the crossover temperature being below 1 K. Then, the following questions need to be addressed: Can we attribute the change of specific heat with temperature to a phonon dimensionality effect? Does it appear with the correct order of magnitude? In the following, we will estimate the Debye 3D model, Debye 2D model, and elastic continuum model (ECM) of specific heat and compare the different orders of magnitude obtained to sort out the various physical mechanisms at play.

The Debye 3D model of specific heat is characterized by its temperature variation following a cubic power law $C \propto T^3$ as given by the formula [27]

$$c_{\mathrm{Debye3D}} = \frac{2\pi^2 k_B^4}{\rho 15 \hbar^3}\left(\frac{2}{v_T^3} + \frac{1}{v_L^3}\right)T^3, \tag{2}$$

where ρ is the mass density in $\mathrm{g/m^3}$, $\hbar$ is the reduced Planck constant, k_B is the Boltzmann constant, and v_T and v_L are the transverse and longitudinal speeds of sound, 6200 and 10 300 m/s, respectively, for silicon nitride [7]; the specific heat c_{Debye3D} is in $\mathrm{J\,g^{-1}\,K^{-1}}$. This model has demonstrated over the years its great ability to fit c_p experimental values of crystalline electrically insulating materials [28,29]. It can be adapted to 2D systems by integrating over the wave vectors parallel to the membrane surface in a planar geometry (keeping the regular longitudinal and transverse 3D bulk phonon modes):

$$c_{\mathrm{Debye2D}} = \frac{3\zeta(3)k_B^3}{\pi\hbar^2}\left(\frac{2}{v_T^2} + \frac{1}{v_L^2}\right)T^2, \tag{3}$$

where ζ is the Riemann zeta function. This area-dependent specific heat in $\mathrm{J\,m^{-2}\,K^{-1}}$ does not depend on the thickness of the 2D membrane and has a lower temperature exponent compared with the Debye 3D model, the power law being given by the dimension of the system. This Debye 2D model is compared with the experimental surface specific heat as measured on SiN membranes in Fig. 3(a). Even if the Debye 2D specific heat is larger than the Debye 3D one, significant

discrepancies still exist. Indeed, the measured absolute value of c_p is in strong disagreement with the calculated ones, being a few orders of magnitude bigger.

A refinement of the model seems necessary. This is done by taking into account the modified phonon modes present in thin membranes. In the following, the specific heat of thin freestanding membranes at low temperature is obtained through the calculation of phonon modes of a phonon cavity using the elastic continuum model [7,9–12]. In this model, some bulk polarizations will couple together at the surfaces generating a new set of vibrational modes: dilatational waves (or symmetric Lamb waves), flexural waves (or asymmetric Lamb waves), and horizontal shear waves [10,11,30]. The modified 2D dispersion relations of these modes have important consequences for the low-temperature specific heat. Again, by integrating over the wave vector parallel to the membrane surface $q_{||}$, the total surface specific heat can be written as

$$c_{\mathrm{ECM}} = \frac{A}{k_B T^2 2\pi} \sum_{\sigma} \sum_{m=0}^{\infty} \int_0^{\infty} dq_{||} \frac{q_{||}(\hbar\omega_{m,\sigma})^2 \exp(\beta\hbar\omega_{m,\sigma})}{[\exp(\beta\hbar\omega_{m,\sigma}) - 1]^2}, \tag{4}$$

where $\beta = (k_B T)^{-1}$, σ represents the different modes, and $\sum_m$ is the summation over all the branches of a mode.

According to the calculations at low enough temperature, for membranes much thinner than λ_{dom}, the contribution of the flexural waves becomes dominant. In contrast to the Debye 2D model, the elastic continuum theory then predicts a linear variation of specific heat (not quadratic) with temperature at very low temperature [7,9,11]. This linear dependence comes from the quadratic dispersion relation of the dominant flexural modes. The temperature at which this 3D-2D crossover appears depends on the thickness of the phonon cavity via the dependence on temperature of the dominant phonon wavelength. The surface specific heat, as evaluated by the ECM, is shown in Fig. 3(a) only above 0.5 K due to its very low value. The measured $c_p(T)$ and the one calculated using the ECM have very dissimilar absolute values showing that the elastic continuum model does not give a good account of what has been measured, being off by a few orders of magnitude.

All of the models we have considered so far are in principle valid only for *crystalline* systems. As SiN thin films are amorphous and disordered, some specific thermal properties may be expected. One of the most important properties of noncrystalline materials is that they contain a large number of two-level systems. Two-level systems are atoms or groups of atoms that have two metastable configurations in their energy landscape. At low enough temperature these atoms or groups of atoms can switch between these two states only by quantum tunneling. An important ingredient when considering the physics of these TLSs is that a uniform and broad spectral distribution for time constants or, equivalently, barrier heights is assumed. The exact origin of these two-level systems is still heavily debated, though they can be seen as extra degrees of freedom in the solid [19,31–37]. At low temperature, phonons can interact strongly with the TLSs, which has consequences not only for the specific heat but also for the phonon thermal transport [4,5,16]. The contribution of the TLSs to the specific heat is given by [15,19,32]

$$c_{\mathrm{TLS}} = \frac{\pi^2}{6} \frac{n_0}{\rho} k_B^2 T = \alpha T, \tag{5}$$

with ρ being the mass density in $\mathrm{g/m^3}$ of the material and n_0 being the density of TLSs; α is in $\mathrm{J\,g^{-1}\,K^{-2}}$. c_{TLS} is the specific heat linked to low-energy excitation specific to glassy materials; it will dominate the c_p signal at low temperature. Another contribution to specific heat in amorphous solids can come from extra nonpropagating modes; this is usually modeled by an excess specific heat having a cubic power law [32]:

$$c_{ex} = \gamma\, T^3, \tag{6}$$

γ being a factor determined experimentally. For most disordered materials, γ lies in the range 1×10^{-7} to $10 \times 10^{-7}\ \mathrm{J\,g^{-1}\,K^{-4}}$. This excess specific heat has been observed in most disordered materials [16,32]. Nonpropagating modes and TLSs are both associated with low-density regions specific to disordered materials where voids or floppy bonds are present. The total specific heat of amorphous materials will be given by the relation $c_{\mathrm{tot}} = c_{\mathrm{TLS}} + c_{ex} = \alpha T + \gamma T^3$.

We can now compare the contribution of these two different mechanisms in disordered solids with the measured specific heat. In Fig. 3(b), we have reported our experimental data for the volumetric specific heat and plotted the theoretical contributions to c_p, the excess specific heat and the specific heat due to two-level systems, as obtained from Eqs. (5) and (6); the prefactors γ in Eq. (6) and the density of two-level systems n_0 in Eq. (5) being the adjustable parameters. We have also plotted data taken by other groups on 50- and 200-nm-thick SiN membranes [16,26]. By comparing the different experimental data, we can first notice that the specific heat we observe is larger by more than two orders of magnitude than the one measured on a-SiN membranes.

In order to reproduce the experimental data using the TLS model, we have to consider the specific heat due to localized soft modes [c_{ex}, Eq. (6)] as well as the specific heat due to two-level systems [c_{TLS}, Eq. (5)], taking for the adjustable parameters $\gamma \approx 10^{-4}\ \mathrm{J\,g^{-1}\,K^{-4}}$ and $n_0 \approx 1.5 \times 10^{49}\ \mathrm{J^{-1}\,m^{-3}}$. Using these parameters, we can reproduce *quantitatively* the experimental data as shown in Fig. 3(b) with the red line fit. The membrane specific heat is dominated over the whole temperature range of the experiment by the amorphous nature of the SiN: Above 1 K, the specific heat is interpreted to be dominated by localized soft modes, whereas in the low-temperature range, the specific heat is almost entirely due to the presence of two-level systems. The density of TLSs in the 100-nm-thick membrane is $n_0 \approx 1.5 \times 10^{49}\ \mathrm{J^{-1}\,m^{-3}}$, a relatively high value as for 300 nm $n_0 \approx 1.5 \times 10^{48}\ \mathrm{J^{-1}\,m^{-3}}$, lying slightly above the measured range in amorphous silicon, $n_0 \approx 10^{44}$–$10^{48}\ \mathrm{J^{-1}\,m^{-3}}$ [32].

To confirm this scenario of TLS-dominated c_p, it is interesting to try to control the density of the two-level systems in the material; this can be done by changing the mass density of the material by the following mechanism: When the composition of SiN is changed, this affects the internal stress along with the mass density. Since the TLSs are thought to result from dangling bonds arising from voids or surfaces, varying

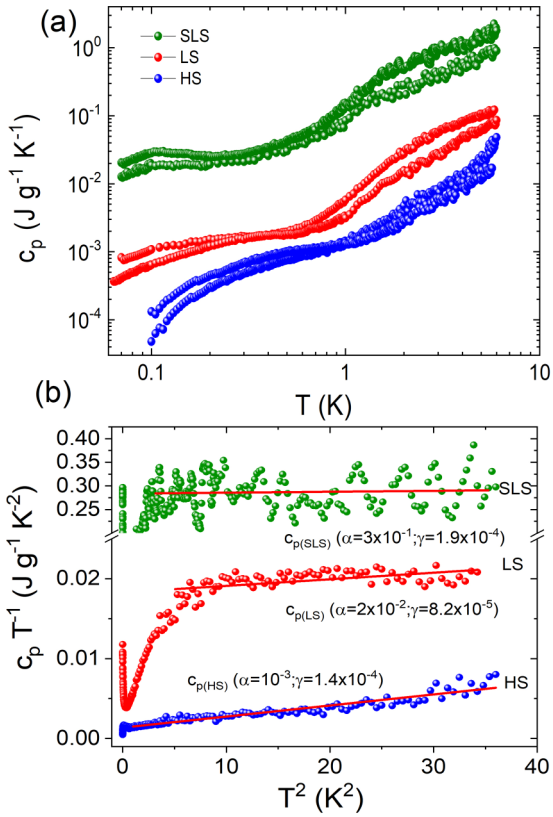

FIG. 4. The temperature dependence of the specific heat for different internal stresses of SiN_x. The samples all have the same geometry with a thickness of 100 nm. The specific heat measurements were done for two sets of membranes of each kind of SiN: Blue, red, and green dots are the specific heat of high-stress (HS), low-stress (LS), and super-low-stress (SLS) amorphous silicon nitride, respectively. In (a) the specific heat vs T is plotted in a log-log scale, and in (b) c_p/T vs T^2 is plotted to highlight the α (intercept with y axis) and γ (the slope of the linear fit) values for each internal stress. The units of α are J g^{-1} K^{-2}, and the units of γ are J g^{-1} K^{-4}.

the mass density and stress should affect the TLS density and with it the specific heat. We consequently expect a higher TLS density in lower-mass-density materials having lower mechanical stress. Therefore we decided to reproduce the same c_p experiments on high-stress (HS), low-stress (LS), and super-low-stress (SLS) amorphous silicon nitride membranes to probe the effect of various TLS densities on the specific heat.

The temperature dependence of the specific heat of the different 100-nm-thick SiN membranes is depicted in Fig. 4. Using Eq. (5), we can extract from our measurements an order of magnitude for the concentration of TLS in our membranes, summarized in Table I. This table displays the composition, the mass density, the TLS density, and the stress for each composition as given by the supplier [38]. The composition and the mass densities were determined by Rutherford backscattering spectrometry (RBS).

The main observation from Fig. 4 is that by decreasing the stress and the mass density between HS and SLS SiN, the specific heat is increased by two orders of magnitude. These values are surprisingly high in comparison to what has

TABLE I. Parameters for high-stress (HS), low-stress (LS), and super-low-stress (SLS) SiN_x. ρ is the mass density of material measured by Rutherford backscattering spectrometry, n_0 is the TLS density of states as extracted from the measurements using Eq. (5), and the stress for each composition is as given by the supplier [38].

SiN_x	HS	LS	SLS
Composition	$Si_{43}N_{57}$	$Si_{46}N_{54}$	$Si_{48}N_{52}$
ρ (g/cm^3)	3.2	2.9	2.4 ± 0.2
n_0 (J^{-1} m^{-3})	1.5×10^{49}	3.6×10^{49}	3.3×10^{50}
Stress (GPa)	0.85	0.2	<0.1

been measured until now on amorphous dielectric materials [19,32,39]. We suppose that such a high value of the specific heat can be attributed to the presence of two-level systems and localized modes in amorphous SiN. One remarkable feature appears when inspecting Table I: It seems that there is a correlation between the density of TLSs and the mass density. Indeed, there is a factor of 20 between the density of TLSs in HS and SLS a-SiN_x. In between these two samples, the mass density varies by >30%. We guess that this variation of mass density is due to the appearance of low-density regions in the amorphous SiN located on the surface; it is precisely these low-density regions which are favorable for the formation of TLSs; this could explain the difference by orders of magnitude in the specific heat between SLS and HS SiN through a much higher TLS density. More investigations will be required to elucidate the true origin of this behavior.

IV. CONCLUSION

In conclusion, we have measured the specific heat of thin SiN membranes from 6 K down to very low temperature (50 mK) to investigate the heat capacity of 2D phonon cavities. In the whole temperature range, the specific heat does not exhibit a single power law as a function of temperature, but a crossover between two different regimes around 1 K. As was suggested first by Gusso and Rego [9], this crossover could have been correlated to a 3D-2D transition when the phonon wavelength became of the order of the thickness of the membrane. However, first, the position of the crossover in terms of temperature is not in agreement with the ECM; it is at too high a temperature. Second, the absolute value of the measured specific heat is much larger than that predicted from our ECM analysis in terms of surface specific heat. This rules out the idea that, in SiN membranes, the contribution of the Lamb modes to c_p can explain such very high values of specific heat. Rather, we have demonstrated that the exceptionally high magnitude of the specific heat likely results from the presence of a large density of two-level systems, as expected for amorphous disordered systems such as the ones used in this paper (SiN membranes). Our modeling indicates that above 1 K the specific heat is dominated by an excess bulklike contribution, possibly due to nonpropagating modes, and that it is dominated by two-level systems at lower temperatures. Using different SiN compositions, we have also shown that by changing the density of two-level systems through the mass density of the SiN material, high values of specific heat can be reached [19,39,40]. The formation

of TLSs is enhanced by the presence of low-density regions in the SiN and by the presence of large surfaces due to the membrane geometry of the samples. These results will have a significant impact on the performance of low-temperature sensors.

ACKNOWLEDGMENTS

The authors are thankful for the technical support provided by the Nanofab, Pôle Capteur, Pôle électronique, and Pôle de cryogénie facilities at Institut Néel. We thank C. Bachelet and C. Marrache-Kikuchi from the Irène Joliot-Curie laboratory, CNRS, for help with the RBS measurements and Boris Brisuda for proofreading. The research leading to these results has received funding from the European Union's Horizon 2020 research and innovation program, under Grant Agreement No. 824109; the European Microkelvin Platform (EMP); the EU project MERGING, Grant No. 309150; and ERC CoG Grant ULT-NEMS No. 647917. The authors also acknowledge the financial support from the ANR project QNM, Grant No. 040401. T.P. and I.M. acknowledge the financial support from Academy of Finland Project No. 341823.

[1] F. Giazotto, T. T. Heikkila, A. Luukanen, A. M. Savin, and J. P. Pekola, Rev. Mod. Phys. **78**, 217 (2006).
[2] K. Schwab, E. A. Henriksen, J. M. Worlock, and M. L. Roukes, Nature (London) **404**, 974 (2000).
[3] N. Zen, T. A. Puurtinen, T. J. Isotalo, S. Chaudhuri, and I. J. Maasilta, Nat. Commun. **5**, 3435 (2014).
[4] A. Tavakoli, C. Blanc, H. Ftouni, K. J. Lulla, A. D. Fefferman, E. Collin, and O. Bourgeois, Phys. Rev. B **95**, 165411 (2017).
[5] A. Tavakoli, K. Lulla, T. Crozes, E. Collin, and O. Bourgeois, Nat. Commun. **9**, 4287 (2018).
[6] D. V. Anghel, J. P. Pekola, M. M. Leivo, J. K. Suoknuuti, and M. Manninen, Phys. Rev. Lett. **81**, 2958 (1998).
[7] T. Kühn, D. V. Anghel, J. P. Pekola, M. Manninen, and Y. M. Galperin, Phys. Rev. B **70**, 125425 (2004).
[8] T. Kühn and I. J. Maasilta, Nucl. Instrum. Methods Phys. Res., Sect. A **559**, 724 (2006).
[9] A. Gusso and L. G. C. Rego, Phys. Rev. B **75**, 045320 (2007).
[10] O. V. Fefelov, J. Bergli, and Y. M. Galperin, Phys. Rev. B **75**, 172101 (2007).
[11] E. Chávez, J. Cuffe, F. Alzina, C. M. Sotomayor Torres, in *6th European Thermal Sciences Conference (Eurotherm 2012) 4–7 September 2012, Poitiers, France*, Journal of Physics: Conference Series Vol. **395**, (Institute of Physics, London, 2012), p. 012105.
[12] T. A. Puurtinen and I. J. Maasilta, AIP Adv. **6**, 121902 (2016).
[13] J. Cuffe, E. Chávez, A. Shchepetov, P. O. Chapuis, E. H. El Boudouti, F. Alzina, T. Kehoe, J. Gomis-Bresco, D. Dudek, Y. Pennec, B. Djafari-Rouhani, M. Prunnila, J. Ahopelto, and C. M. Sotomayor Torres, Nano Lett. **12**, 3569 (2012).
[14] W. A. Phillips, J. Low Temp. Phys. **7**, 351 (1972).
[15] P. W. Anderson, B. I. Halperin, and C. M. Varma, Philos. Mag. **25**, 1 (1972).
[16] R. O. Pohl, X. Liu, and E. Thompson, Rev. Mod. Phys. **74**, 991 (2002).
[17] D. R. Southworth, R. A. Barton, S. S. Verbridge, B. Ilic, A. D. Fefferman, H. G. Craighead, and J. M. Parpia, Phys. Rev. Lett. **102**, 225503 (2009).
[18] H. Ftouni, C. Blanc, D. Tainoff, A. D. Fefferman, M. Defoort, K. J. Lulla, J. Richard, E. Collin, and O. Bourgeois, Phys. Rev. B **92**, 125439 (2015).
[19] J. Wu and C. C. Yu, Phys. Rev. B **84**, 174109 (2011).
[20] O. Bourgeois, D. Tainoff, A. Tavakoli, Y. Liu, M. Boukhari, A. Barski, and E. Hadji, C. R. Phys. **17**, 1154 (2016).
[21] T. D. Nguyen, A. Tavakoli, S. Triqueneaux, R. Swami, A. Ruhtinas, K. Hasselbach, A. Frydman, B. Piot, M. Gibert, E. Collin, and O. Bourgeois, J. Low Temp. Phys. **197**, 348 (2019).
[22] O. Bourgeois, S. E. Skipetrov, F. Ong, and J. Chaussy, Phys. Rev. Lett. **94**, 057007 (2005).
[23] G. M. Souche, J. Huillery, H. Pothier, P. Gandit, J. I. Mars, S. E. Skipetrov, and O. Bourgeois, Phys. Rev. B **87**, 115120 (2013).
[24] S. Poran, M. Molina-Ruiz, A. Gérardin, A. Frydman, and O. Bourgeois, Rev. Sci. Instrum. **85**, 053903 (2014).
[25] S. Poran, T. Nguyen-Duc, A. Auerbach, N. Dupuis, A. Frydman, and O. Bourgeois, Nat. Commun. **8**, 14464 (2017).
[26] D. R. Queen and F. Hellman, Rev. Sci. Instrum. **80**, 063901 (2009).
[27] A. N. Cleland, *Foundations of Nanomechanics* (Springer-Verlag, Berlin, 2003).
[28] H. M. Rosenberg, *Low Temperature Solid State Physics*, (Clarendon, Oxford, 1965).
[29] E. S. R. Gopal, *Specific Heats at Low Temperatures* (Springer-Verlag, Berlin, 1966).
[30] K. F. Graff, *Wave Motion in Elastic Solids*, (Oxford University Press, Oxford, 1991).
[31] D. R. Queen, X. Liu, J. Karel, T. H. Metcalf, and F. Hellman, Phys. Rev. Lett. **110**, 135901 (2013).
[32] D. R. Queen, X. Liu, J. Karel, T. H. Metcalf, and F. Hellman, J. Non-Cryst. Solids **426**, 19 (2015).
[33] B. L. Zink, R. Pietri, and F. Hellman, Phys. Rev. Lett. **96**, 055902 (2006).
[34] B. L. Zink and F. Hellman, Solid State Commun. **129**, 199 (2004).
[35] A. J. Leggett, Phys. B (Amsterdam) **169**, 322 (1991).
[36] A. J. Leggett and D. C. Vural, J. Phys. Chem. B **117**, 12966 (2013).
[37] V. Lubchenko, Adv. Phys.: X **3**, 1510296 (2018).
[38] The SiN/Si wafers were purchased from Si-Mat (https://www.si-mat.com/en/).
[39] R. O. Pohl, in *Amorphous Solids: Low-Temperature Properties*, edited by W. A. Phillips (Springer-Verlag, Berlin, 1981), pp. 27–52.
[40] T. Pérez-Castañeda, R. J. Jimenez-Rioboo, and M. A. Ramos, Phys. Rev. Lett. **112**, 165901 (2014).